T.M. Harrell, O.T. Thomsen, J.M. Dulieu-Barton, and S.F. Madsen, "Damage in CFRP Composites Subjected to Simulated Lighting Strikes - Assessment of Thermal and Mechanical Responses," Composites Part B: Engineering, 2019.
https://doi.org/10.1016/j.compositesb.2019.107298

Damage in CFRP Composites Subjected to Simulated Lighting Strikes - Assessment of Thermal and Mechanical Responses

T.M. Harrell[1a], O.T. Thomsen[1], J.M. Dulieu-Barton[1] and S. F. Madsen[2]

[1]School of Engineering and Physical Sciences, University of Southampton, Highfield Campus, SO17 1BJ, UK
[2]PolyTech A/S, Hedehusene, Denmark
[a]T.M.Harrell@soton.ac.uk

Abstract

Damage is inflicted upon Carbon Fiber Reinforced Polymer (CFRP) composite laminates using simulated lightning strikes to investigate the resulting residual mechanical properties. Seven different CFRP laminate specimens were exposed to simulated lightning strikes using three different electric waveforms. The three waveforms imposed were the 10/350 µs waveform, which simulates the first return stroke during a direct strike according to IEC 61400-24 Ed1.0. The second was a unipolar long stroke component, and the third was a combination of the first return stroke and the long stroke. After exposure to lightning, coupon specimens were prepared for mechanical testing. The test specimens were subsequently subjected to compression and shear loading to determine the post-strike mechanical properties. The compression tests were conducted using uniaxial coupons in accordance with ASTM standard D6641. The shear tests were conducted using V-notch specimens utilizing an Iosipescu test rig in accordance with ASTM standard D5379. Digital Image Correlation was used to capture the strain fields on the surface of the specimens. The results of the material coupon tests are compared with test results from pristine CFRP coupon samples that were not exposed to any electrical current. The shear and compression

strengths, compressive and shear stress-strain curves, compressive and shear moduli, and the maximum temperature on the CFRP specimens during lightning tests are presented and discussed. Key results include that the largest reduction of strength occurred in the specimens that were subjected to the largest current and specific energy. The specific energy correlated more closely to the observed reduction of residual strength than the charge, and the damaged specimens displayed a higher degree of nonlinear stress-strain behavior than the pristine specimens.

Keywords

CFRP composites; Lightning Damage; Wind Turbine Blades; Compression and Shear Testing; Thermal Imaging; Digital Image Correlation (DIC); Failure Initiation Stress

1 INTRODUCTION

Lightning protection of wind turbine (WT) blades has received significant attention as most wind blade manufacturers now feature blade designs that include conductive Carbon Fiber Reinforced Polymer (CFRP) composites for structural components. Previously, the leading designs predominately used non-conductive Glass Fiber Reinforced Polymer (GFRP) composites for structural components, hence the change in design has created a new set of challenges when dealing with lightning strike damage. CFRP materials, which are stiff, strong, and lightweight, are also effectively semi-conductors with strong anisotropic electrical and thermal properties. Thus, CFRP materials exhibit properties different from other conductive engineering materials, e.g. metal alloys, making CFRPs more susceptible to lightning damage. The main reasons for this are the limited electrical and thermal conductivities transverse to the fibers, the

anisotropic material properties, and the integration of the CFRP into the overall WT blade or aerospace structures. Lightning strikes can lead to damage in CFRP materials from elevated temperatures which result in loss of resin, fiber breakage, and delamination [1].

With the progressive use of CFRP materials in WT blade structures, it is important to develop a full understanding of the effects of lightning strike induced damage on the material and the structural response. There are several documented cases, where a lightning strike has been the cause of premature WT blade failure [2]. For example, a 2012 report by the insurance company GCube Insurance [3] states that almost a quarter (23.4%) of damage to WT blades in the USA reported to GCube was caused by lightning.

The aerospace industry has implemented CFRP materials into structural components for decades, and has explored different methods of reducing and/or mitigating the damage introduced by lightning interacting with CFRP materials. Much of the literature focuses on direct effects from an arc entry direct lightning strike [4]–[8] because this is the most common scenario of electric current injection into CFRP on aircraft structures. In WTs, arc entry (or direct lightning strike) occurs on occasion, but the more common exposure is conducting current from the so-called ‘down conductors’ i.e. a metallic wire (usually made of copper) which is placed between the two WT CFRP sparcaps. This wire conducts the electric current to ground. However, the CFRP laminate also introduces another conductive path. The current will use both the down conductor and the CFRP to conduct the electrical current to ground. Down conductors are typically bonded to the CFRP to prevent internal flashovers between the down conductor and the CFRP. A

flashover is an event where electrical current conducts through the air between two conductors; in this case, the down conductor and the CFRP. Left unbonded the voltage will continue to increase along the length of the blade leaving the blade vulnerable to internal flashovers. An example of a typical blade with a lightning protection system and the electric current path is shown in **Fig. 1**. The typical lightning protection system (LPS) consists of a cylindrical metallic conductor, connected to the air termination system and to the carbon fiber laminate of the blade structure. The LPS connects the down conductor to the root of the blade with the nacelle.

The current levels generated by lightning in the CFRP can cause material and structural damage due to thermal heating from the Joule (or resistive) heating response. The effects of a direct lightning strike on the mechanical behavior and performance of CFRP materials have been investigated previously [9]–[12], and only one investigation [13] has previously considered CFRPs subjected to conducted current scenarios. No previous research has studied the effects of lightning damage on the material properties dominated by the polymer matrix including the shear and compression loading responses.

The research presented in the present paper investigates the reduction or degradation of the mechanical properties of CFRP laminates caused by a simulated lighting strike, where the CFRP laminates investigated are representative of materials used in current WT blade structures. This paper focuses on the effects of simulated lightning strike induced damage on the load response and failure behavior of CFRP laminates subjected to shear and compression loading.

T.M. Harrell, O.T. Thomsen, J.M. Dulieu-Barton, and S.F. Madsen, “Damage in CFRP Composites Subjected to Simulated Lighting Strikes - Assessment of Thermal and Mechanical Responses,” Composites Part B: Engineering, 2019.
https://doi.org/10.1016/j.compositesb.2019.107298

2 METHODOLOGY

2.1 Specimen Manufacturing

Eight CFRP unidirectional (UD) five ply laminate specimens were manufactured using the carbon/epoxy material system PX-35 from Zoltek. The eight laminates were manufactured using vacuum liquid resin infusion producing strips with dimensions of 500 mm long x 50 mm wide x 4.5 mm thick. The specimens were chamfered at the ends with an approximate 1:4 taper to expose the carbon fibers and provide a connection point. Silver conductive paint and copper plate were added to the tapered sections to aid in conducting the electric current to the exposed fibers. The volume fraction of the material was estimated from micrographs to be 57%, which is consistent with typical values for the VARTM process. **Fig. 2** shows an example of the manufactured CFRP strips.

2.2 Simulated Lightning Strike Experiments

The CFRP strip specimens were subjected to electrical current with three different waveforms. The first waveform examined was a unipolar 10/350µs waveform simulating the first return stroke during a direct strike according to IEC 61400-24 Ed1.0 [14]. The second being a unipolar long stroke component (or DC) also defined by the IEC standards. The third waveform being a combination of the 10/350µs and DC waveform. All of the current components were tested using the conducted current test method provided in Annex D3.4 of IEC 61400-24 Ed1.0 [14]. An example of the test setup and the current path during the testing is shown in **Fig. 3**.

The initial stroke waveform was an impulse which is defined by three characteristic parameters; the peak current value (I_{peak}), the rise time to reach the peak current (t_1), and the time at which the current decays to half of the peak current (t_2), also known as the half time. The DC current is defined by the peak current value (I_{peak}), and the duration (t_{DC}), and these parameters are shown in **Fig. 4**. The charge, C, and the specific energy or action integral, AI, are used to compare different waveforms and are calculated as follows:

$$C = \int_0^{t_f} i(t)\, dt \tag{1}$$

and

$$AI = \int_0^{t_f} i^2(t)\, dt \tag{2}$$

where t_f is the final current time, and $i(t)$ is the current level at any time t.

Table 1 provides an overview of the characteristic parameters used in the lightning strike tests. These comprise of three different waveforms that are considered representative of the exposure experienced by WT blades in operation: DC, Impulse, and Impulse+DC.

During the simulated lightning strike experiments, an infrared camera was used to capture the thermal evolutions. The infrared camera was a PYROVIEW 640L, which is an uncooled micro-bolometer array with 640 × 480 pixels. The maximum image capture rate of 50 Hz was used. The camera captured one full surface of the specimen. The post-processing of the thermal data was based on data captured from the middle of the CFRP specimens (about 40% of the specimen width). This was done to ensure that influence

from the connections and any flame ignition had only a small or little influence on the results. All thermal data from the middle of the specimen was averaged at each captured thermal image (frame) to gather a temperature evolution over time. This was done to remove outliers and determine the temperatures experienced by the material testing coupons.

2.3 Compression and Shear Coupon Test Specimens

Compression and shear tests were conducted according to ASTM D6641 [15] (compression) and ASTM standard D5379 [16] (Iosipescu V-notch test), respectively. The coupon specimens were manufactured by waterjet cutting from the vacuum infused CFRP strips. The layout of the test specimen waterjet cutting scheme is shown in **Fig. 5**.

The compression test specimens were 10 mm wide x 150 mm long and were mounted with end tabs made of S-glass with a 1:4 tapered section. The end tabs were bonded to the specimens using Araldite 4858. An example of the compression sample is shown in **Fig. 6** (a). The compression tests were conducted using an Instron 100 kN servo-hydraulic test machine with a loading rate of 0.2 mm/min in accordance with ASTM D6641 [15].

An example of the Iosipescu V-notch shear test specimens is shown in **Fig. 6** (b). The shear tests were conducted using an Instron 50 kN electro-mechanical test machine with a loading rate of 0.5 mm/min in accordance with ASTM standard D5379 [16].

Four control specimens that had not been subjected to simulated lightning strikes were also tested in compression and shear. Three damaged specimens from each test

configuration (see **Table 1**) were tested in both compression and shear. A total of 50 tests were conducted; 25 in compression and 25 in shear. The obtained results for the lightning strike damaged specimens were compared to the results obtained for the pristine (undamaged) CFRP specimens. **Table 2** summarizes the adopted test matrix.

2.4 Digital Image Correlation

Digital Image Correlation (DIC) was used to obtain full field measurement of the strains on the specimen surface during testing. As the specimens were already black, they were coated with only a thin layer of black paint to make a uniform surface and then speckled with white paint as opposed to the more conventional white background with black speckles; this ensured the paint coating was thin, so the damage was not filled by the paint coating. Images were captured with an 'E-Lite LaVision' camera equipped with a Sigma 105mm lens. The load levels were recorded from the test machine as the images were captured simultaneously using the software package DaVis [17]. The experimental setup is shown in **Fig. 7**. The DIC was processed through the DaVis correlation software to determine the strains. The post-processing used a substep size of 55 x 55 pixels and a step size of 21.

To determine the adequacy of the DIC measurements, strain gauges were mounted on the back side of the control samples. A 350 Ohm linear pattern strain gauge (CEA-06-250UW-350) was used for the compression test specimens, and a 350 Ohm shear pattern strain gauge (EA-06-062TV-350) was used for the shear specimens. The data collected using strain gauges showed a good correlation with the DIC measurements; see **Fig. 8**. The maximum difference between the measurements obtained using the two

techniques was assessed by calculating the Young's or shear moduli from the linear regression lines drawn through the origin of the coordinate axes. The largest difference was found to be less than 4%. Due to the good correlation, DIC was used for the remainder of the tests ensuring any resin lost during due to the lightning damage was not filled by the adhesive bonding necessary for the strain gauge attachment.

For the DIC measurements, a Region of Interest (ROI) was defined in the gauge sections of the specimens as shown in **Fig. 9**. The DIC data was post-processed by taking the mean of the strains measured over the ROI. For the compression tests, the strains were averaged over 50% of the gauge section length. This was done for the ROI to avoid stress concentration due to load introduction from the end tabs. For the shear specimens, the strains were averaged over the whole gauge section was used for the ROI as proposed by [18], [19]. The averaged strains measured over the ROI zones were referenced against the average (or nominal) stresses in the gauge zone defined by the force measured by the load cell divided by the gauge zone cross section areas.

2.5 Determination of Failure Initiation Stress

When conducting the tests, it was important to determine at what stress/strain levels damage initiated in the specimens. To assess this, the methodology devised by [20], [21] was employed. The method assumes that the total strain measure can be split into an elastic part and an inelastic part as follows:

$$\varepsilon = \varepsilon_e + \varepsilon_i \tag{1}$$

where the elastic part is $\varepsilon_e = \sigma/E$, and the 'inelastic' part is assumed to follow the nonlinear relation:

$$\varepsilon_i = a \ln\left(1 - \left(\frac{\sigma}{\sigma_0}\right)^m\right) \tag{2}$$

which is often adopted for the modelling of metal alloy plasticity [20].

In Eqs. (1) and (2), E is the Young's modulus, σ_0 is the horizontal asymptote of the stress-strain curve, the parameter m relates to a strain hardening rule of the material, and a scales the magnitude of the inelastic strains. It should be noticed that, in this work, the inelastic strain ε_i accounts for the cumulative effects of (resin/matrix) plasticity, micro-cracks and geometrically nonlinear effects due to fiber rotations etc. Therefore, the fitting parameter m does not represent strain hardening in any physical sense, and the expression for ε_i is merely to be seen as a nonlinear fitting law. Following this, an appropriate definition of onset point of damage/nonlinearity can be adopted as occurring when the gradient of the tangential stiffness changes sign. Following this the 'failure initiation stress' can be defined as suggested in [21]:

$$\frac{d^3\sigma}{d\varepsilon^3} = 0. \tag{3}$$

The stress-strain response of the V-notch shear specimens is significantly influenced by the matrix material and therefore can be expected to exhibit substantial nonlinearity, whereas the compression tests are expected to display a more linear stress-strain response. Accordingly, the methodology outlined for estimating the onset of nonlinearity, defined as the failure initiation strength, was only used for the shear tests. The data fitting was carried out by a least squares method and implemented in the commercial software Maple 2017 [22].

3 RESULTS

Seven of the manufactured CFRP strips were subjected to simulated lightning strike events. Three specimens were subjected to long stroke direct current and labelled ‘DC’ in **Table 1**, and three specimens were subjected to a unipolar current and labelled ‘Impulse’ in **Table 1**. Finally, one specimen was subjected to a combined impulse and long stroke and was labelled ‘Impulse+DC’ in **Table 1**. The resistance of the CFRP strips was large (200 mΩ over 50 cm) and the Impulse waveform achieved was a 15/110µs waveform. For resin infused products porosity is a concern, hence the material was manufactured following the same procedure as for the wind turbine blade manufacture. The results from the Control mechanical test indicated strongly that there was little porosity as the Young’s modulus values were close to the values provided in the Nordex data sheet. X-ray Micro-CT scans at a resolution of 900 nm confirmed that there was no visible porosity in the material in three of the CFRP test specimens (Control, DC3 and Impulse3).

3.1 Damage Introduction

The temperature evolution during the DC, Impulse, and Impulse+DC tests were similar, as shown by images captured by the infrared camera in **Fig. 10**, where the temperature increase is distributed evenly throughout the samples. The largest increase in temperature corresponded to the largest specific energy used in the lightning tests. The DC tests yielded very little audible acoustic response and led to little or no visual indication of damage of the specimens. In contrast, the Impulse and Impulse+DC tests

were much louder and rapid events with bright flames emitting from the current injection points that dissipated within a few seconds.

The images shown in **Fig. 10** were captured using a Nikon digital SLR camera and a PYROVIEW 640L infrared camera. **Fig. 10** splices white light images (Nikon) on the left with the thermal images (PYROVIEW) on the right. The white light images had an exposure time of 5 seconds that allowed the accumulation of light intensity to be captured throughout the tests. The thermal images were taken from the image frame immediately after the lightning strike test or where the maximum heating of the specimens occurred.

During the DC tests there were no visual indications of suspected damage in the white light images captured and as shown on the right in **Fig. 10** (a) the infrared image displays a uniform increase in temperature. The Impulse tests also showed no visual indication of damage despite the appearance of sparks and flames as described above. In **Fig. 10** (b), the white light image on the left does show flames and sparks, but these are products of air ignition between the metallic contact point and the CFRP testing material, as the combustion temperature of the CFRP was not reached. This is confirmed in the thermal images captured after the dissipation of the flames. These show a uniform temperature increase in the sample both where the flames appeared at the contact points, as well as in the middle where no flames appeared. The Impulse+DC tests displayed more extensive visual indication of damage, with flames engulfing the sample and lasting several seconds longer than end of the current supplied to the sample; see **Fig. 10** (c). In these tests, the combustion point of the specimens was

reached, igniting the epoxy matrix. Although all of the samples showed increases in temperature only one sample, Impulse+DC, showed visible signs of damage.

The thermal data was recorded to find the maximum temperature during the lightning strike tests. The temperature data recorded at the center of the specimens is shown in **Fig. 11**. The thermal data results show that the maximum temperature always occurred after all the current was injected. This data can determine which CFRP specimens went above the glass transition temperature of 79°C for the resin system tested, and how long the specimens were above the glass transition temperature. The DC2-3, Impulse2-3 and Impulse+DC specimens all reached temperatures above the glass transition temperature for extended periods of time. Impulse+DC reached a temperature, which caused ignition of the sample and caused the sample to burn during the test. The apparent second peak of the Impulse+DC at 11s is due to flames that extinguished in the frame of the measurement.

3.2 Visual Inspection

The damaged specimens were inspected visually to assess the damage inflicted to the CFRP materials. The focus of the inspection was to identify fiber, resin, and delamination damage apparent on the surface. The visual inspection was conducted by eye both with and without a 10x magnification optical loupe to allow for a more detailed assessment of the surface. On the DC and Impulse specimens damage was concentrated near the connection points. For the DC and Impulse specimens, the only visible damage found was underneath the connection points, with the likely cause being the transfer from metallic connection to the CFRP, and on specimen Impulse3 within a

distance of 2 cm from the connection point. Selected images from the DC3 and Impulse3 specimens are shown in **Fig. 12**. In the areas where the coupons were cut out, see **Fig. 12** (a) and (b), the material showed no visual signs of damage. Further, **Fig. 12** (c) shows what a typical cross section looks like for all the Impulse and DC samples. This typical cross section has no signs of damage, and there are no visible bulges on the top surface to suggest internal delamination damage. In **Fig. 12** (d) the image shows damaged fibers, loss of resin, and glass fiber stitching from the dry fabric pulled away from the specimen close to the connection point. Therefore, the coupons used in the mechanical tests were cut from regions away from the connection point as indicated in **Fig. 12** (a) and (b).

The Impulse+DC specimen shown in **Fig. 13** displays extensive damage. Both the top and bottom surfaces show resin damage from the flames burning the laminate, as indicated in **Fig. 13** (a). Almost all the cross section has exposed fibers and stitching as shown in **Fig. 13** (b). The resin in between the layers has burnt away which can be seen from the outer surface of the cross section, see **Fig. 13** (c). **Fig. 13**(d) and clearly shows delaminated plies.

3.3 Residual Strength

After the simulated lighting strike tests, the coupon specimens were cut out, and the compression and shear tests described above were carried out. The tests were conducted to failure of the specimen to capture the residual (or remaining) strength after specimens were exposed to the lightning strike damage. The stress was calculated on the gross cross-sectional area before damage. All specimens failed in the gauge section and

displayed acceptable compression or shear failure modes as prescribed in the ASTM standards.

The mean strengths of the compression and shear test specimens that were subjected to lightning strikes were compared to the strengths obtained for pristine/undamaged specimens labeled 'control'. The strength reduction of the damaged specimens relative to the pristine/undamaged specimens are calculated by equation (4):

$$\%\, Reduction = \left(\frac{(\sigma,\tau)_{control}-(\sigma,\tau)_{sample}}{(\sigma,\tau)_{control}} - 1\right) 100\% \quad (4)$$

where $(\sigma,\tau)_{control}$ is the compression/shear failure stress of the undamaged specimen and $(\sigma,\tau)_{sample}$ is the compression/shear failure stress of the damaged specimen.

Table 3 shows the results obtained for the CFRP specimens loaded in compression. The negative % Reduction means that the mean compressive strength was slightly larger than the control samples but is within the overall noise of the test setup. **Table 4** shows the results obtained for the CFRP specimens loaded in shear.

From **Table 3** and **Table 4** it is observed that the measured residual strengths are reduced only moderately for the DC and Impulse specimens. However, the Impulse+DC case represents the most severe simulated lightning strike action on a small cross section, and much more severe strength reductions are seen, with 71.4% reduction for the compression specimens, and 43% for the shear specimens.

3.4 Residual Modulus

The Young's (E) and shear moduli (G) for both damaged and pristine specimens were also evaluated from the test data following the procedures outlined in ASTMD6641 [14] and ASTMD5379 [15]. The results are shown in **Fig. 14**, and it is observed that only moderate changes to E and G were experienced for the DC and Impulse specimens. However, the Impulse+DC specimens showed significant reductions in both Young's (E) and shear moduli (G). The residual compressive modulus is reduced to almost a third of its pristine/undamaged value.

3.5 Stress Strain Relationship

The stress vs. strain relations were also recorded for all the test specimens, and typical stress-strain curves are shown in **Fig. 15** for the compression tests, and in **Fig. 16** for the shear tests. A significant change of the stress-strain response is observed for all cases (i.e. DC, Impulse and Impulse+DC), even for the DC and Impulse specimens where the residual strengths and moduli only changed modestly as shown in **Table 3** and **Table 4** and **Fig. 14**. In particular, it is observed that as the lightning strike energy level increases, the nonlinearity of the stress-strain response as well as the strain to failure increases. The former suggests that the failure initiation shear strength of the CFRP specimens, as defined in section 2.5 and Eqs. (1-3), reduces with increasing lightning strike energy levels.

3.6 Failure Initiation Stress

The failure initiation stress values, as defined in section 2.5 and Eq. (1-3), for the shear test specimens are shown in **Table 5**.

The failure initiation strength provides a quantitative measure of the stress where nonlinear stress-strain behavior initiates. It is observed from **Table 5** that this reduces significantly even for DC and Impulse simulated lightning strike events that led to modest changes of (initial) stiffness (E and G) and compressive/shear strengths (see section 3.3 and 3.4), and where only limited visual damage could be identified. For the worst case scenario of the Impulse+DC simulated lightning strike event, is it also clear from **Table 5** that significant damage has been introduced. The initiation point of nonlinear behavior/response has been reduced by 60%, for that specimen. This reduction can be seen in **Fig. 15** and **Fig. 16**, as well as in **Table 4** which shows a significant reduction in shear strength.

4 DISCUSSION

The research presented proposes a procedure with results to evaluate the damage inflicted to CFRP materials from exposure to a severe simulated lightning strike event. The series of simulated lightning strike tests conducted represent common exposure (Impulse 1-3 and DC 1-3) to overly exposed (Impulse+DC) lightning situations experienced by WT blades manufactured using CFRP composite materials. The samples tested were scaled down versions of a typical sparcap. The tests conducted aimed at exposing the CFRP samples with lightning current, providing a certain degree of damage (reduction of residual strength). The current magnitudes and hence current

densities chosen may be exceeding the actual exposure for profiles being part of a real sparcap in a wind blade. To compare the results of the present tests with the exposure of actual blades in service, the current densities for the actual sparcap geometry must be carefully assessed by analysis or current distribution testing according to IEC 61400-24 Ed2. This means that the Impulse1-3 specimens were struck with a maximum current of 60 kA; this scales to an average cross-section (500mm x 5mm) to have a similar current density level on the specimen as a typical WT blade sparcap exposed to a “Lightning Protection Level 1” or LPL1 from the IEC61400-24 wind turbine lightning standard [14]. The DC1-3 specimens were made to match the Impulse1-3 action integrals (AI) to a maximum of 200 C. The combine Impulse+DC case is an extreme case which is not a realistic lightning strike scenario but shows the full damage which can be caused in a CFRP material when exposed to a large amount of electrical current.

During a lightning strike event, the CFRP material typically can experience significant heating exceeding glass transition or combustion temperatures. For CFRP materials that have been exposed to lightning strikes that cause combustion/burning, significant damage will be inflicted including loss of loss of resin, fiber breakage, and delamination. This in turn can lead to significant changes (reductions) of the mechanical response of the material, demonstrated by the findings described in the previous section of this paper. Similar results show that CFRP materials exposed to fire (i.e. exposure to elevated temperatures) can experience a significant loss of strength and stiffness with a clear correlation to their mass loss [23]. This indicates that thermal effects and degradation play a large role in determining the influence of lightning induced damage on the strength, stiffness and overall load response of CFRP materials.

The strong correlation between sample temperature and the severity of a lightning strike event is indicated in **Fig. 17**, which shows the surface temperature rise measured on the CFRP specimens using an infrared camera, and the charge and specific energy associated with the specific simulated lightning strike tests conducted.

It is observed from **Fig. 17** that the Impulse+DC tests conducted led to far higher specimen temperatures than the DC and Impulse tests, indicating much more damage being inflicted during the former. This corresponds very well with the results presented in sections 3.3 to 3.6 where it was shown that the Impulse+DC tests inflicted very significant damage leading to large reductions of strength, stiffness, and failure initiation strength.

Although the visual inspections conducted on the DC and Impulse coupon tests did not reveal any significant damage, the mechanical tests revealed that both types of simulated lightning strikes reduced the strength for both the compression and shear load cases. This trend can be identified by evaluating the (residual) compression and shear strength measured for the CFRP specimens that did not combust (i.e. DC1-3 and Impusle1-3) against charge, see **Fig. 18**, and specific energy, see **Fig. 19**, of the simulated lightning strike. From **Fig. 18** and **Fig. 19** it is observed that the specific energy appears to have a stronger effect in reducing the residual strengths than the charge of the lightning strike event. It should also be noted that even though the simulated lightning strike waveforms displayed large variations with respect to the amount current and charge injected into the specimens, it is clear that the both the DC and Impulse test specimens display a clear strength reduction correlation with respect to the specific energy.

T.M. Harrell, O.T. Thomsen, J.M. Dulieu-Barton, and S.F. Madsen, “Damage in CFRP Composites Subjected to Simulated Lighting Strikes - Assessment of Thermal and Mechanical Responses,” Composites Part B: Engineering, 2019.
https://doi.org/10.1016/j.compositesb.2019.107298

5 CONCLUSIONS

The results of a comparative investigation of the damage induced by a lightning strike through conducted current in CFRP materials has been presented. The focus of this investigation has been to measure the residual mechanical properties of CFRP specimens post lightning strike, as well as the recording of the temperature evolution during simulated lightning strike events. In addition to visual inspection, the mechanical testing encompassed assessment of the residual compression strength, the shear strength and the material stiffnesses (Young’s and shear moduli), measured using ASTM standard test methods, as well as estimation of the overall change of stress-strain response due to lightning strike.

Seven CFRP strips were subjected to simulated lighting strike events characterized by three different waveforms considered representative for the exposure experienced by WT blades in operation: DC, Impulse, and Impulse+DC. The recorded temperatures and the mechanical tests have shown that the most significant damage was induced to the CFRP specimens, which experienced the highest temperature and combustion/burning.

The compression tests showed that impulse current has a more severe impact on the compression strength than DC current, with a strength reduction of approximately 19% caused by a 60 kA 10/110µs waveform (10 Coulomb). In comparison, a 7% reduction of the compression strength was observed for the case of a 0.75 kA long duration (200 Coulomb) DC current. There was little difference between the effects caused by impulse and DC currents on the shear strength with 7-8% reduction for both the impulse and long duration currents.

T.M. Harrell, O.T. Thomsen, J.M. Dulieu-Barton, and S.F. Madsen, “Damage in CFRP Composites Subjected to Simulated Lighting Strikes - Assessment of Thermal and Mechanical Responses,” Composites Part B: Engineering, 2019. https://doi.org/10.1016/j.compositesb.2019.107298

The most severe damage was inflicted by combined impulse and DC currents (Impulse+DC), which resulted in reductions of the compression strength of more than 70% and more than 40% for the shear strength.

6 ACKNOWLEDGMENT

This work was sponsored by the Marie Skłodowska Curie Actions, Innovative Training Networks (ITN), Call: H2020-MSCA-ITN-2014, as part of the 642771 “Lightning protection of wind turbine blades with carbon fiber composite materials” SPARCARB project. The mechanical testing described in the paper was conducted in the Testing and Structures Research Laboratory (TSRL) at the University of Southampton https://www.southampton.ac.uk/engineering/research/facilities/360/tsrl_360.page. The authors are grateful for the support received from Dr. Andy Robinson, the TSRL Principal Experimental Officer.

7 REFERENCES

[1] L. Chemartin *et al.*, “Direct Effects of Lightning on Aircraft Structure : Analysis of the Thermal , Electrical and Mechanical Constraints,” *J. Aerosp. Lab*, no. 5, pp. 1–15, 2012.

[2] Y. Yasuda, S. Yokoyama, M. Minowa, and T. Satoh, “Classification of lightning damage to wind turbine blades,” *IEEJ Trans. Electr. Electron. Eng.*, vol. 7, no. 6, pp. 559–566, 2012.

[3] GCubeInsurance, “GCube Top 5 US Wind Energy Insurance Claims Report,” 2012. [Online]. Available: http://www.gcube-insurance.com/press/gcube-top-5-us-wind-energy-insurance-claims-report/.

[4] P. Feraboli and M. Miller, “Damage resistance and tolerance of carbon/epoxy composite coupons subjected to simulated lightning strike,” *Compos. Part A Appl. Sci. Manuf.*, vol. 40, no. 6–7, pp. 954–967, 2009.

[5] T. Ogasawara, Y. Hirano, and A. Yoshimura, “Coupled thermal-electrical analysis for carbon fiber/epoxy composites exposed to simulated lightning current,” *Compos. Part A Appl. Sci. Manuf.*, vol. 41, no. 8, pp. 973–981, 2010.

T.M. Harrell, O.T. Thomsen, J.M. Dulieu-Barton, and S.F. Madsen, “Damage in CFRP Composites Subjected to Simulated Lighting Strikes - Assessment of Thermal and Mechanical Responses,” Composites Part B: Engineering, 2019. https://doi.org/10.1016/j.compositesb.2019.107298

[6] G. W. Reid, “Investigations Into the Damage for Various Types of Unprotected Carbon Fibre Composites With a Variety of Lightning Type Arc Attachments,” in *International Conference on Lightning & Static Electricity*, 1991, p. 11.

[7] P. Feraboli and H. Kawakami, “Damage of Carbon/Epoxy Composite Plates Subjected to Mechanical Impact and Simulated Lightning,” *J. Aircr.*, vol. 47, no. 3, pp. 999–1012, 2010.

[8] S. Kamiyama, Y. Hirano, T. Okada, and T. Ogasawara, “Lightning strike damage behavior of carbon fiber reinforced epoxy, bismaleimide, and polyetheretherketone composites,” *Compos. Sci. Technol.*, vol. 161, no. February, pp. 107–114, 2018.

[9] C. Karch and W. Wulbrand, “Thermo-Mechanical Damage of Protected CFRP Structures Caused by Lightning Continuous Currents,” in *International Conference on Lightning & Static Electricity*, 2013, pp. 1–12.

[10] B. Lepetit, F. Soulas, S. Guinard, I. Revel, and G. Peres, “Analysis of composite panel damages due to a lightning strike: mechanical effects.,” in *International Conference on Lightning & Static Electricity*, 2013, pp. 1–8.

[11] C. Karch, J. Steinwandel, K. W. Dittrich, and R. Honke, “Contributions of lightning current pulses to mechanical damage of CFRP structures,” in *International Conference on Lightning & Static Electricity (ICOLSE 2015)*, 2015, no. May, p. 2 (8 .)-2 (8 .).

[12] T. M. Harrell, O. T. Thomsen, S. F. Madsen, and L. Carloni, “Lightning protection of CFRP wind turbine blades - What is the dominant cause of failure : Specific Energy or Charge?,” in *International Conference on Lightning and Static Electricity*, 2017, pp. 1–5.

[13] G. W. Reid, “Strength degradation of CFC due to conduction of simulated lightning currents with varying moisture content and mechanical loading,” in *International Conference on Lightning & Static Electricity*, 1989, pp. 1–8.

[14] International Electrotechnical Commission, “IEC61400: Wind turbine standard,” 2014.

[15] ASTMD6641, *Standard Test Method for Compressive Properties of Polymer Matrix Composite Materials Using a Combined Loading Compression (CLC) Test Fixture*. 2016.

[16] ASTMD5379, *Standard Test Method for Shear Properties of Composite Materials by the V-Notched Beam Method*. 2012.

[17] LaVision, *DaVis 8.3 User Manual*. 2012.

[18] S. C. Hung and K. M. Liechti, “Finite Element Analysis of the Arcan Specimen for Fiber Reinforced Composites under Pure Shear and Biaxial Loading,” *J. Compos. Mater.*, vol. 33, no. 14, pp. 1288–1317, 1999.

[19] F. Pierron and A. Vautrin, “Measurement of the in-plane shear strengths of

unidirectional composites with the Iosipescu test,” *Compos. Sci. Technol.*, vol. 57, no. 12, pp. 1653–1660, Jan. 1998.

[20] R. M. Christensen, “Observations on the definition of yield stress,” *Acta Mech.*, vol. 196, no. 3–4, pp. 239–244, 2008.

[21] S. Laustsen, E. Lund, L. Kühlmeier, and O. T. Thomsen, “Interfibre Failure Characterisation of Unidirectional and Triax Glass Fibre Non-Crimp Fabric Reinforced Epoxy Laminates,” *Appl. Compos. Mater.*, vol. 22, no. 1, pp. 51–79, 2014.

[22] Maplesoft, *Maple 2017 User Manual*. 2017.

[23] J. Wolfrum, S. Eibl, and L. Lietch, “Rapid evaluation of long-term thermal degradation of carbon fibre epoxy composites,” *Compos. Sci. Technol.*, vol. 69, no. 3–4, pp. 523–530, 2009.

T.M. Harrell, O.T. Thomsen, J.M. Dulieu-Barton, and S.F. Madsen, “Damage in CFRP Composites Subjected to Simulated Lighting Strikes - Assessment of Thermal and Mechanical Responses,” Composites Part B: Engineering, 2019.
https://doi.org/10.1016/j.compositesb.2019.107298

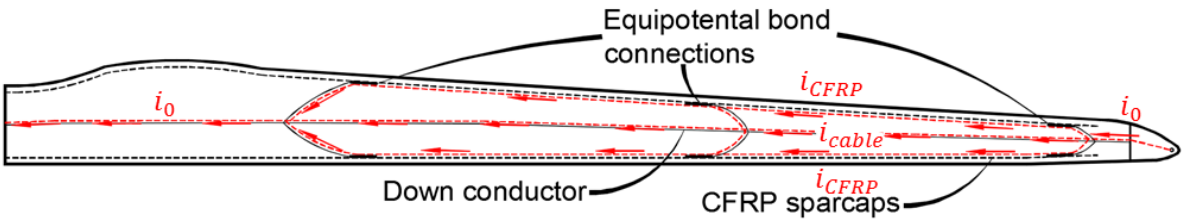

Fig. 1. Wind turbine blade with lightning protection system

T.M. Harrell, O.T. Thomsen, J.M. Dulieu-Barton, and S.F. Madsen, “Damage in CFRP Composites Subjected to Simulated Lighting Strikes - Assessment of Thermal and Mechanical Responses,” Composites Part B: Engineering, 2019. https://doi.org/10.1016/j.compositesb.2019.107298

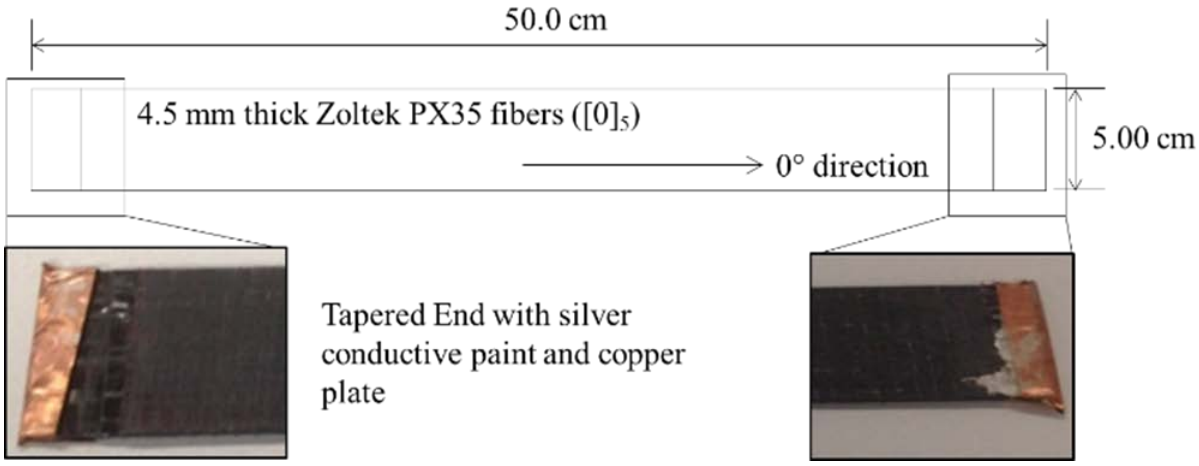

Fig. 2. CFRP strip specimen with dimensions and plating used in simulated lightning strike experiment

T.M. Harrell, O.T. Thomsen, J.M. Dulieu-Barton, and S.F. Madsen, “Damage in CFRP Composites Subjected to Simulated Lighting Strikes - Assessment of Thermal and Mechanical Responses,” Composites Part B: Engineering, 2019. https://doi.org/10.1016/j.compositesb.2019.107298

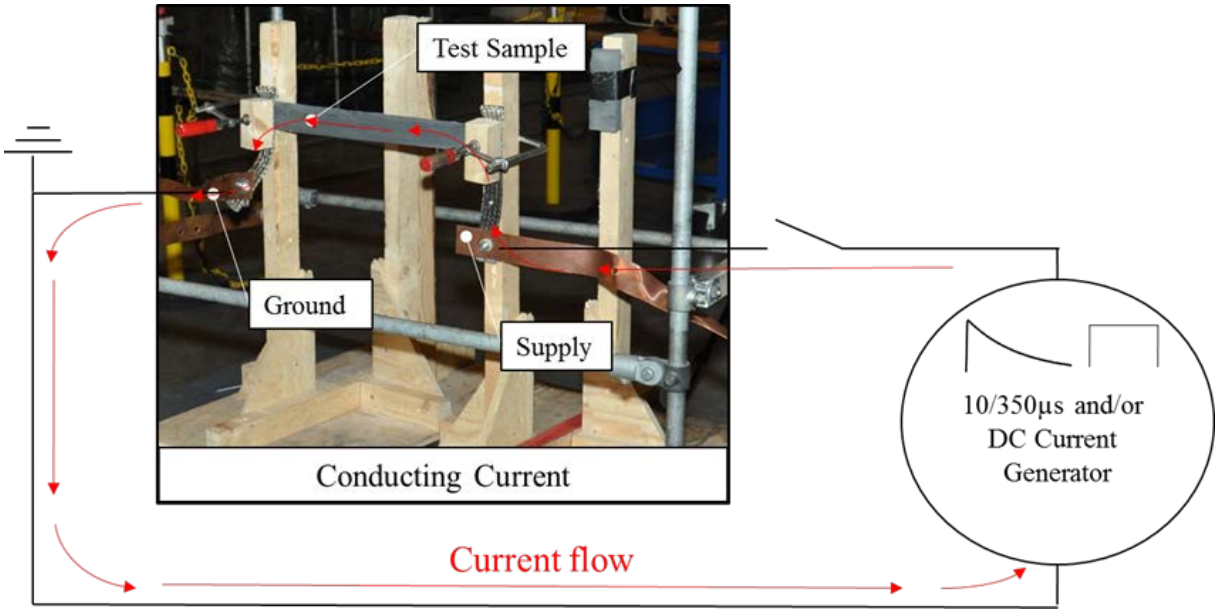

Fig. 3. Electrical circuit describing the current introduction into the CFRP sample through conducted current superimposed on an image of the experimental setup

T.M. Harrell, O.T. Thomsen, J.M. Dulieu-Barton, and S.F. Madsen, “Damage in CFRP Composites Subjected to Simulated Lighting Strikes - Assessment of Thermal and Mechanical Responses,” Composites Part B: Engineering, 2019.
https://doi.org/10.1016/j.compositesb.2019.107298

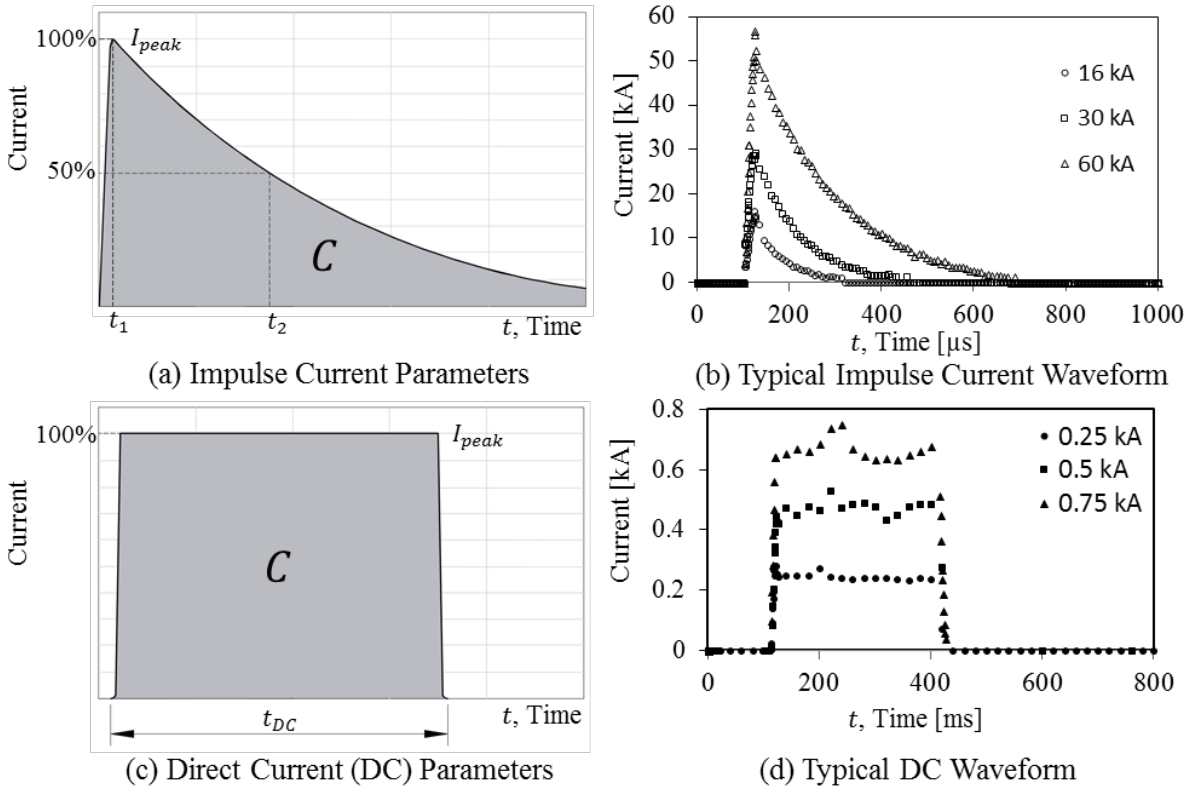

Fig. 4. Lightning strike waveform with parameters for (a-b) impulse waveform characterization, and (c-d) DC waveform characterization

T.M. Harrell, O.T. Thomsen, J.M. Dulieu-Barton, and S.F. Madsen, “Damage in CFRP Composites Subjected to Simulated Lighting Strikes - Assessment of Thermal and Mechanical Responses,” Composites Part B: Engineering, 2019.
https://doi.org/10.1016/j.compositesb.2019.107298

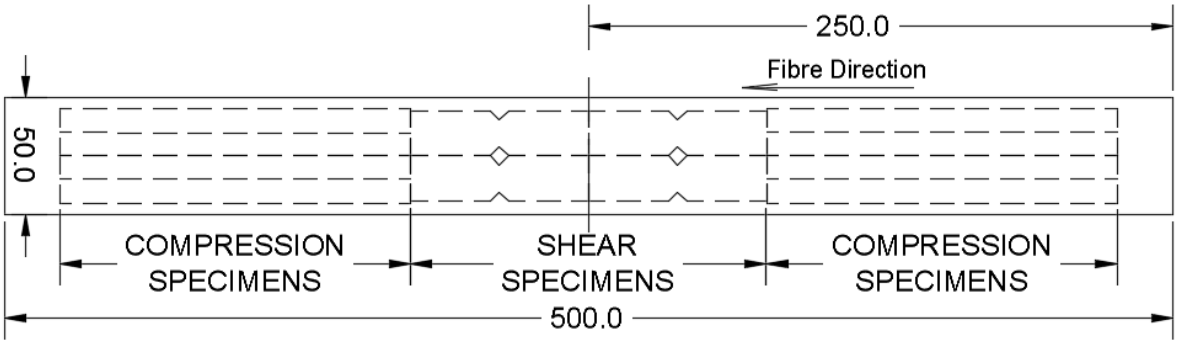

Fig. 5. Waterjet cutting scheme for CFRP compression and shear test specimens

T.M. Harrell, O.T. Thomsen, J.M. Dulieu-Barton, and S.F. Madsen, “Damage in CFRP Composites Subjected to Simulated Lighting Strikes - Assessment of Thermal and Mechanical Responses,” Composites Part B: Engineering, 2019. https://doi.org/10.1016/j.compositesb.2019.107298

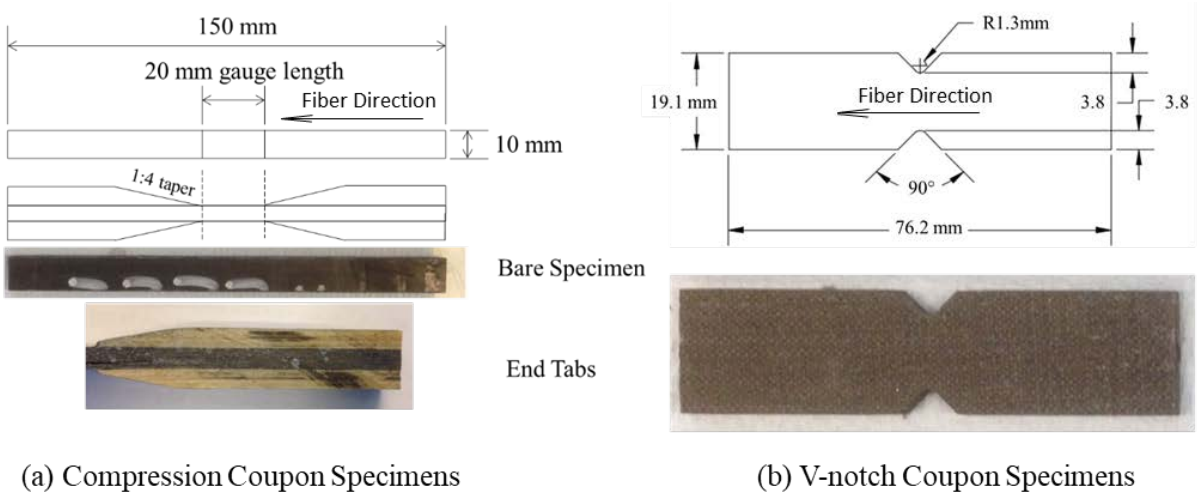

(a) Compression Coupon Specimens (b) V-notch Coupon Specimens

Fig. 6. (a) Compression specimen dimensions and image of a typical sample (b) shear specimen dimensions and image of a typical sample

T.M. Harrell, O.T. Thomsen, J.M. Dulieu-Barton, and S.F. Madsen, “Damage in CFRP Composites Subjected to Simulated Lighting Strikes - Assessment of Thermal and Mechanical Responses,” Composites Part B: Engineering, 2019. https://doi.org/10.1016/j.compositesb.2019.107298

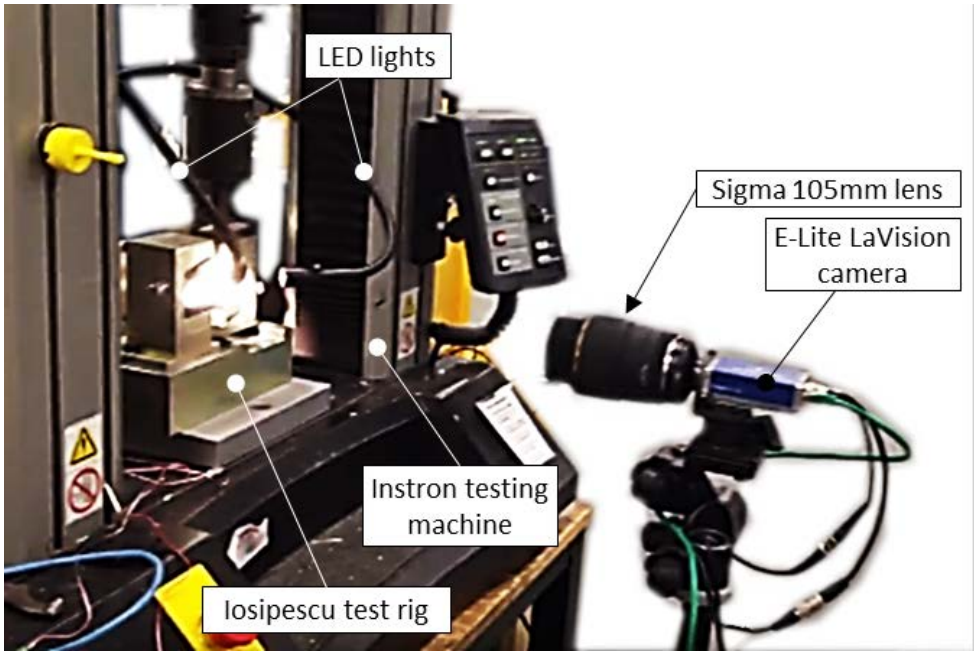

Fig. 7. Experimental setup for Iosipescu tests

T.M. Harrell, O.T. Thomsen, J.M. Dulieu-Barton, and S.F. Madsen, “Damage in CFRP Composites Subjected to Simulated Lighting Strikes - Assessment of Thermal and Mechanical Responses,” Composites Part B: Engineering, 2019.
https://doi.org/10.1016/j.compositesb.2019.107298

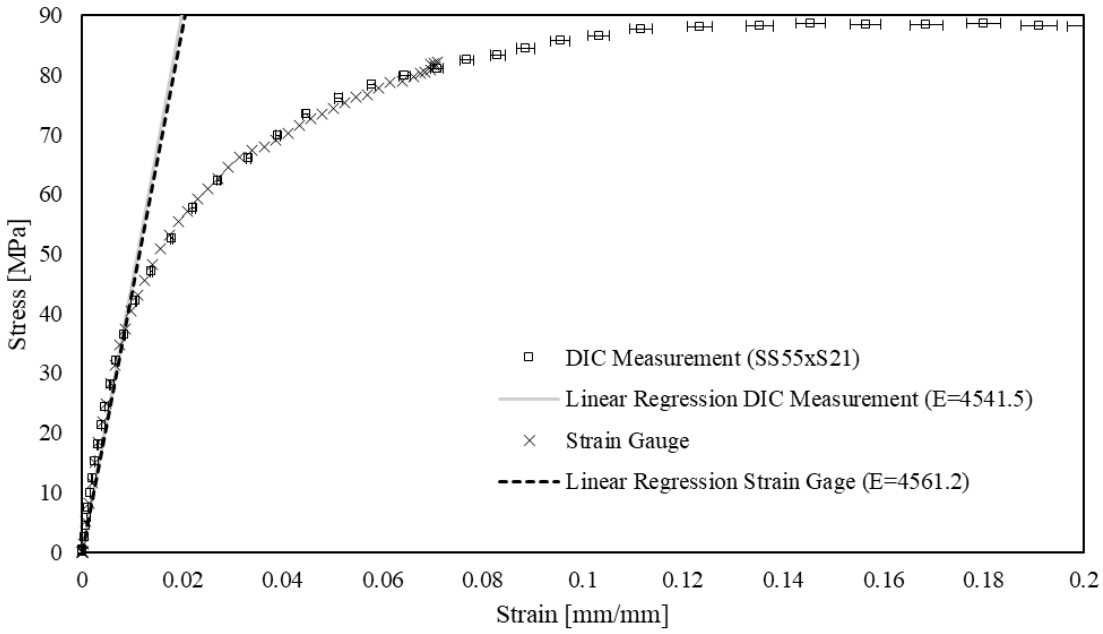

Fig. 8. Strain gauge and DIC comparison

T.M. Harrell, O.T. Thomsen, J.M. Dulieu-Barton, and S.F. Madsen, “Damage in CFRP Composites Subjected to Simulated Lighting Strikes - Assessment of Thermal and Mechanical Responses,” Composites Part B: Engineering, 2019. https://doi.org/10.1016/j.compositesb.2019.107298

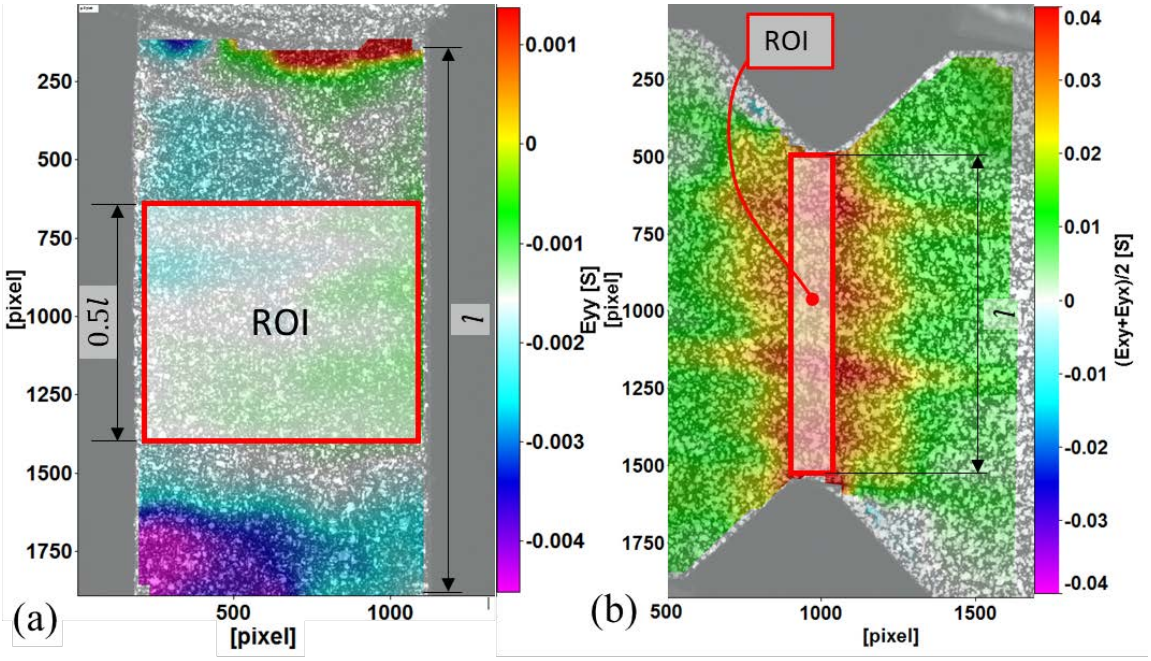

Fig. 9. Example of DIC ROIs: (a) compression specimen, and (b) shear V-notch specimen with an overlay of the ROI area used to calculate the average compression and shear strains

T.M. Harrell, O.T. Thomsen, J.M. Dulieu-Barton, and S.F. Madsen, “Damage in CFRP Composites Subjected to Simulated Lighting Strikes - Assessment of Thermal and Mechanical Responses,” Composites Part B: Engineering, 2019.
https://doi.org/10.1016/j.compositesb.2019.107298

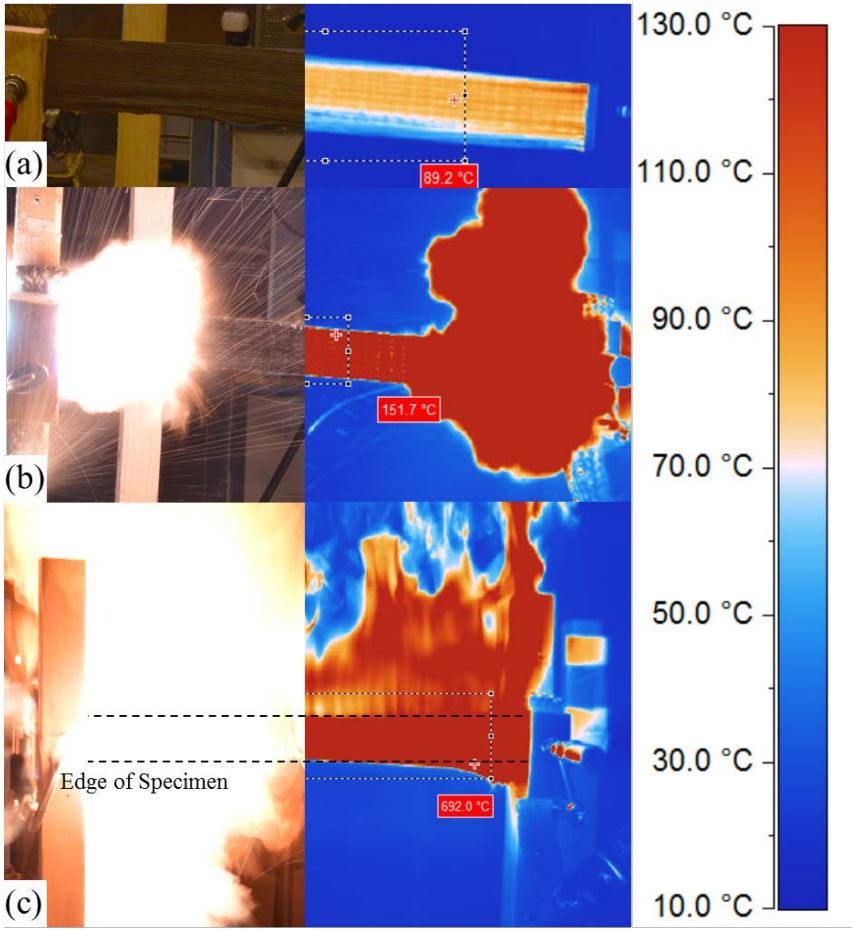

Fig. 10. Selected photos and thermal images from: (a) DC tests, (b) Impulse test, and (c) Impulse+DC test

T.M. Harrell, O.T. Thomsen, J.M. Dulieu-Barton, and S.F. Madsen, “Damage in CFRP Composites Subjected to Simulated Lighting Strikes - Assessment of Thermal and Mechanical Responses,” Composites Part B: Engineering, 2019.
https://doi.org/10.1016/j.compositesb.2019.107298

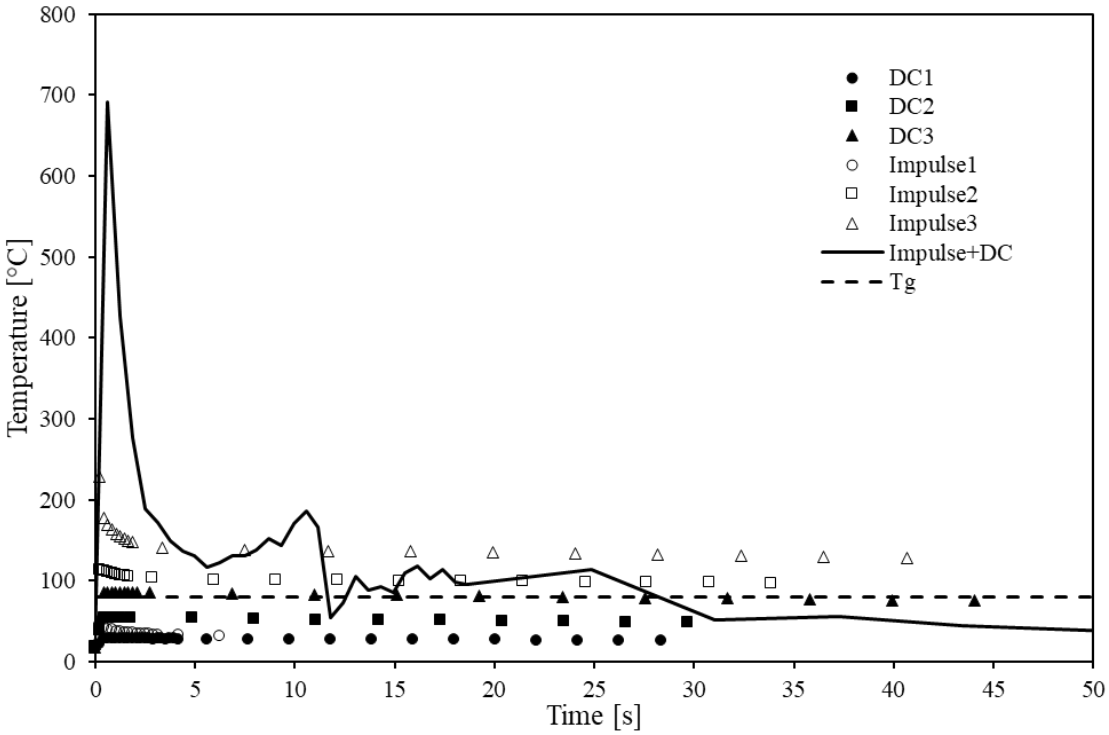

Fig. 11. Average temperature measured at the center of the specimens during lightning strike tests

T.M. Harrell, O.T. Thomsen, J.M. Dulieu-Barton, and S.F. Madsen, “Damage in CFRP Composites Subjected to Simulated Lighting Strikes - Assessment of Thermal and Mechanical Responses,” Composites Part B: Engineering, 2019.
https://doi.org/10.1016/j.compositesb.2019.107298

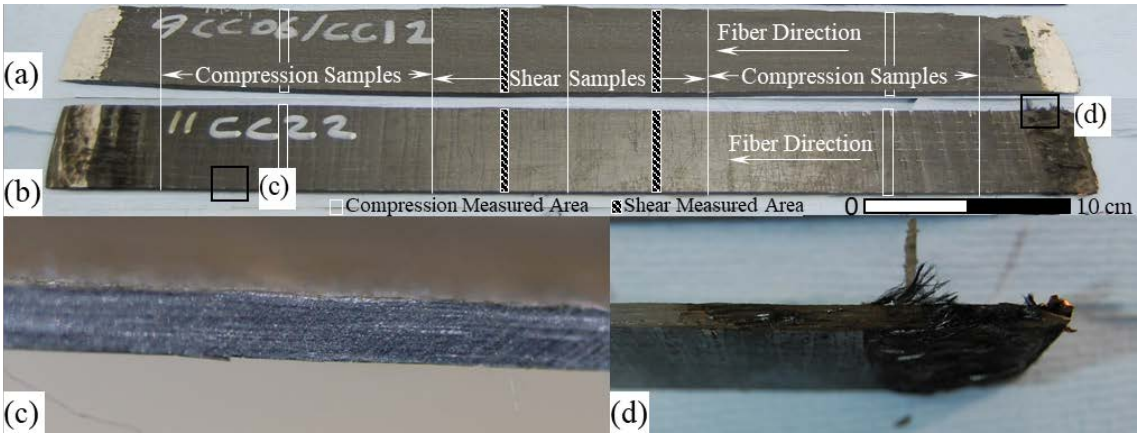

Fig. 12. DC (a) and Impulse (b) post lightning strike damaged specimens with selected cross section images showing (c) typical non-damaged cross section observed for all DC and Impulse specimens (the image shows specimen Impulse3) and (d) damage cross-section close to the connection point (< 2cm) of the Impulse3 specimen

T.M. Harrell, O.T. Thomsen, J.M. Dulieu-Barton, and S.F. Madsen, “Damage in CFRP Composites Subjected to Simulated Lighting Strikes - Assessment of Thermal and Mechanical Responses,” Composites Part B: Engineering, 2019. https://doi.org/10.1016/j.compositesb.2019.107298

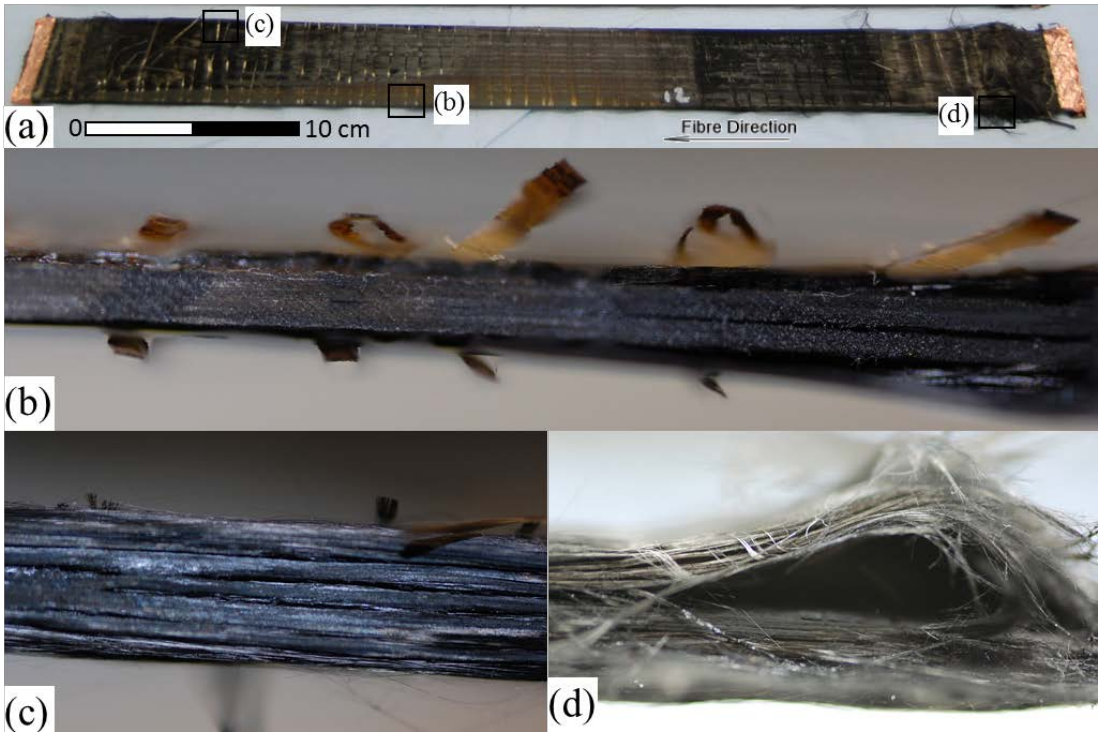

Fig. 13. Impulse+DC: (a) post lightning strike damage specimens with selected cross section images showing typical damage cross section with (b) glass fiber stitching pulled away from the laminate, (c) typical damaged cross-section, and (d) most severely damaged cross section damage close (> 2 cm) to the connection point

T.M. Harrell, O.T. Thomsen, J.M. Dulieu-Barton, and S.F. Madsen, “Damage in CFRP Composites Subjected to Simulated Lighting Strikes - Assessment of Thermal and Mechanical Responses,” Composites Part B: Engineering, 2019.
https://doi.org/10.1016/j.compositesb.2019.107298

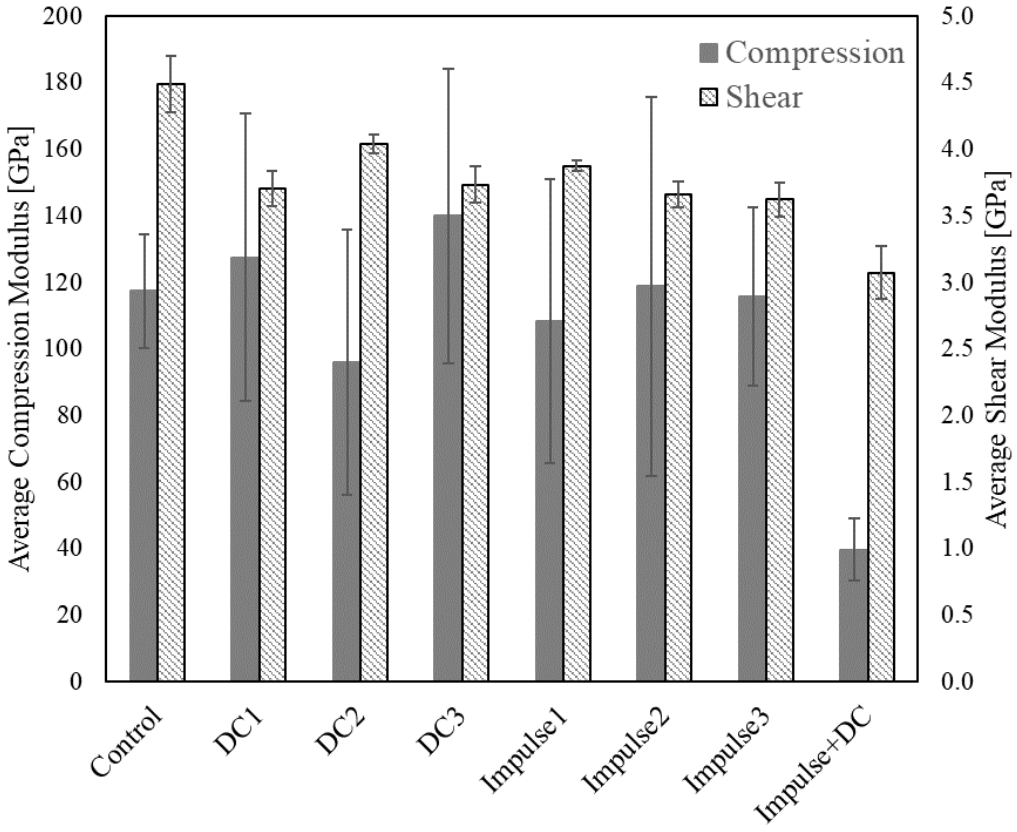

Fig. 14. Residual compression and shear modulus based on specimen waveform

T.M. Harrell, O.T. Thomsen, J.M. Dulieu-Barton, and S.F. Madsen, “Damage in CFRP Composites Subjected to Simulated Lighting Strikes - Assessment of Thermal and Mechanical Responses,” Composites Part B: Engineering, 2019.
https://doi.org/10.1016/j.compositesb.2019.107298

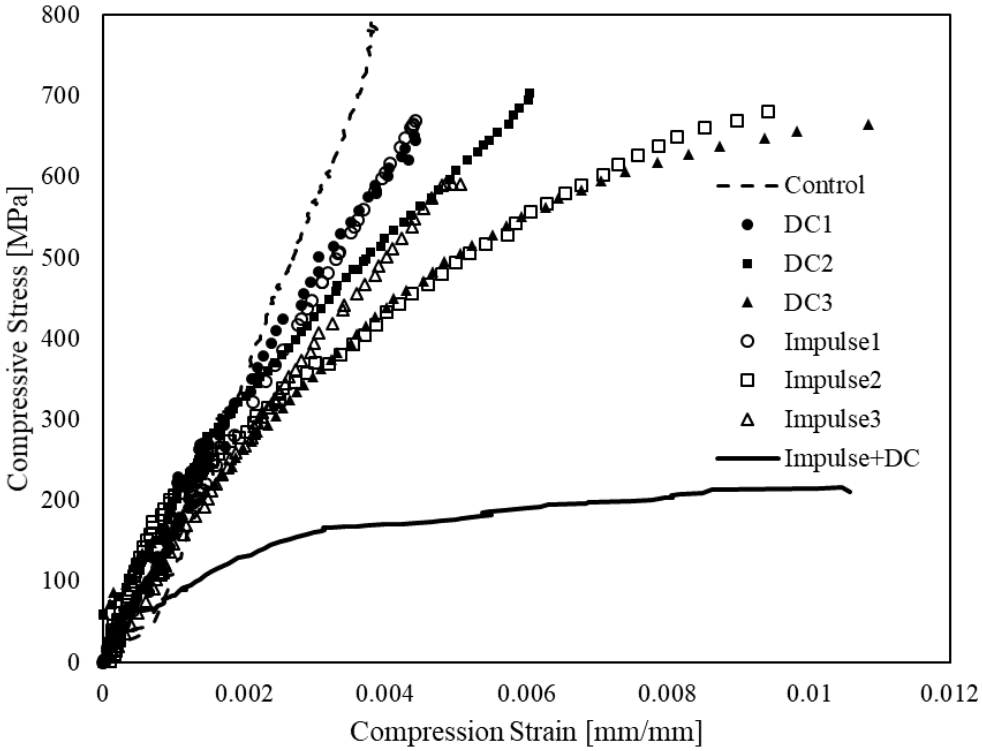

Fig. 15. Typical stress-strain curves recorded for compression specimens

T.M. Harrell, O.T. Thomsen, J.M. Dulieu-Barton, and S.F. Madsen, “Damage in CFRP Composites Subjected to Simulated Lighting Strikes - Assessment of Thermal and Mechanical Responses,” Composites Part B: Engineering, 2019.
https://doi.org/10.1016/j.compositesb.2019.107298

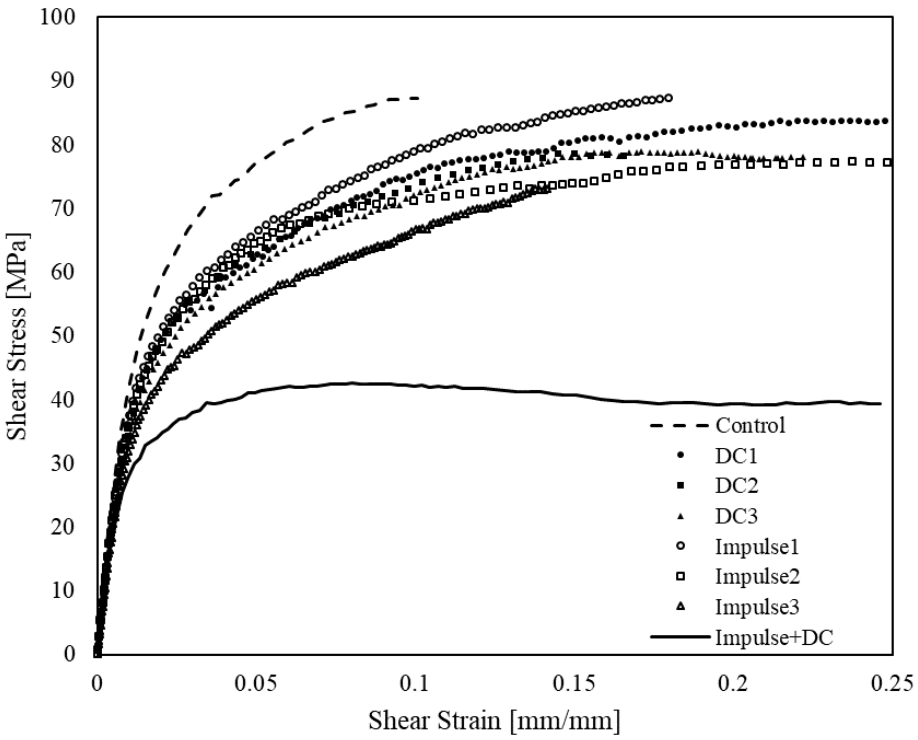

Fig. 16. Typical stress-strain curves recorded for shear specimens

T.M. Harrell, O.T. Thomsen, J.M. Dulieu-Barton, and S.F. Madsen, “Damage in CFRP Composites Subjected to Simulated Lighting Strikes - Assessment of Thermal and Mechanical Responses,” Composites Part B: Engineering, 2019.
https://doi.org/10.1016/j.compositesb.2019.107298

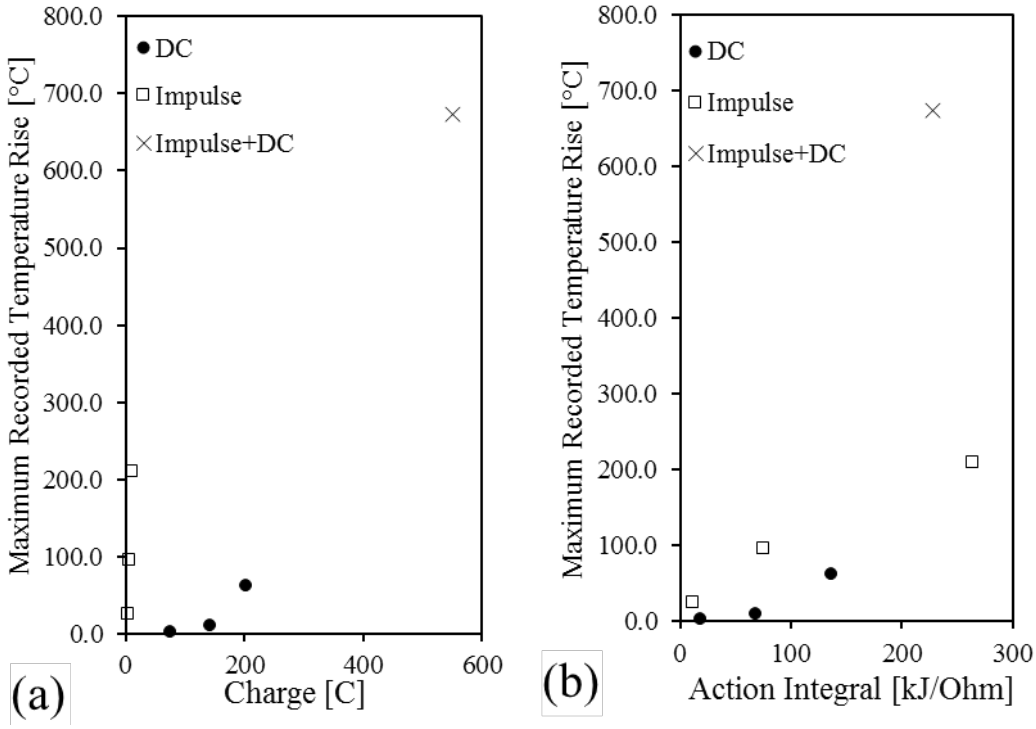

Fig. 17. Maximum temperature rise measured on the CFRP specimen surfaces using vs. (a) charge and (b) action integral (specific energy) associated with specific simulated lightning strike tests

T.M. Harrell, O.T. Thomsen, J.M. Dulieu-Barton, and S.F. Madsen, “Damage in CFRP Composites Subjected to Simulated Lighting Strikes - Assessment of Thermal and Mechanical Responses,” Composites Part B: Engineering, 2019. https://doi.org/10.1016/j.compositesb.2019.107298

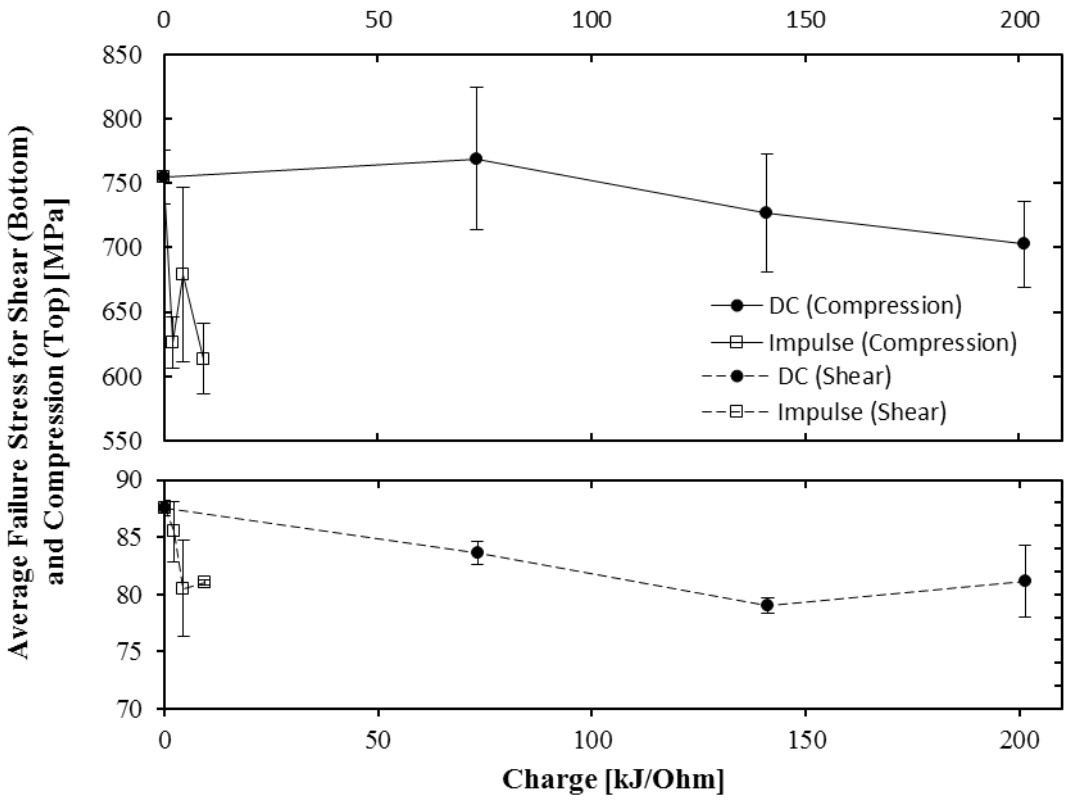

Fig. 18. Residual Strength of damaged and undamaged CFRP specimens vs. charge

T.M. Harrell, O.T. Thomsen, J.M. Dulieu-Barton, and S.F. Madsen, “Damage in CFRP Composites Subjected to Simulated Lighting Strikes - Assessment of Thermal and Mechanical Responses,” Composites Part B: Engineering, 2019.
https://doi.org/10.1016/j.compositesb.2019.107298

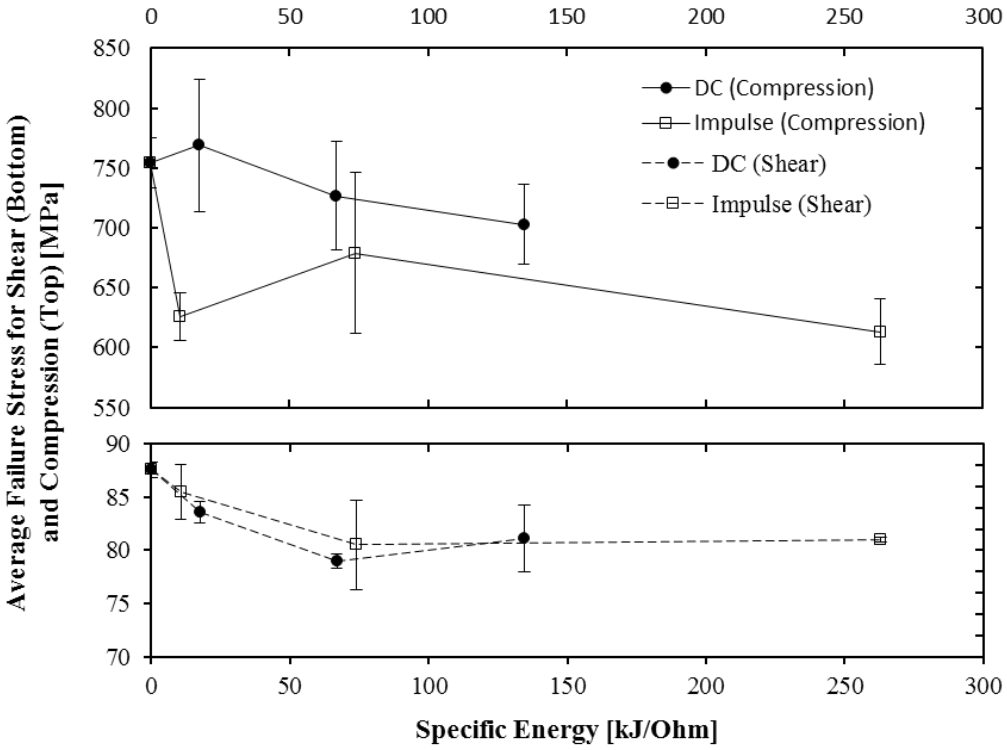

Fig. 19. Residual Strength of damaged and undamaged CFRP specimens vs. specific energy

T.M. Harrell, O.T. Thomsen, J.M. Dulieu-Barton, and S.F. Madsen, “Damage in CFRP Composites Subjected to Simulated Lighting Strikes - Assessment of Thermal and Mechanical Responses,” Composites Part B: Engineering, 2019.
https://doi.org/10.1016/j.compositesb.2019.107298

Table 1. Test parameters defined for the simulated lightning strike tests: Peak amperage, waveform, charge, and specific energy applied to the specimens

Specimen	Peak Amp [kA]	Waveform Characterization (Impulse t_1/t_2) (DC t_{DC})	Charge [C]	AI [kJ/Ohm]
DC1	0.293	314.4	73.2	17.59
DC2	0.531	317.6	141.1	66.94
DC3	0.753	319.6	201.3	134.5
Impulse1	16.2	15.8/50.8	2.13	10.61
Impulse2	34.4	14.6/88.0	4.46	73.9
Impulse3	56.8	15.4/128.8	9.29	263
Impulse+DC	51.5(1)	15.8/110 (622)	8.1 (540.1)	227(498)

T.M. Harrell, O.T. Thomsen, J.M. Dulieu-Barton, and S.F. Madsen, “Damage in CFRP Composites Subjected to Simulated Lighting Strikes - Assessment of Thermal and Mechanical Responses,” Composites Part B: Engineering, 2019. https://doi.org/10.1016/j.compositesb.2019.107298

Table 2. Test matrix for compression and shear coupon tests

Residual Strength Specimen	Type	Nominal Thickness [mm]	Gauge Width [mm]	Repetitions
Control-C	Compression	4.8	10	4
DC1-C	Compression	4.8	10	3
DC2-C	Compression	4.8	10	3
DC3-C	Compression	4.8	10	3
Impulse1-C	Compression	4.8	10	3
Impulse2-C	Compression	4.8	10	3
Impulse3-C	Compression	4.8	10	3
Impulse+DC-C	Compression	4.8	10	3
Control-S	Shear	4.8	11.5	4
DC1-S	Shear	4.8	11.5	3
DC2-S	Shear	4.8	11.5	3
DC3-S	Shear	4.8	11.5	3
Impulse1-S	Shear	4.8	11.5	3
Impulse2-S	Shear	4.8	11.5	3
Impulse3-S	Shear	4.8	11.5	3
Impulse+DC-S	Shear	4.8	11.5	3

T.M. Harrell, O.T. Thomsen, J.M. Dulieu-Barton, and S.F. Madsen, “Damage in CFRP Composites Subjected to Simulated Lighting Strikes - Assessment of Thermal and Mechanical Responses,” Composites Part B: Engineering, 2019. https://doi.org/10.1016/j.compositesb.2019.107298

Table 3. Compression test results of control specimen and damaged specimens showing

Specimen	Mean Compression Strength [MPa]	Standard Deviation [MPa]	% Reduction
Control	754.7	20.9	-
DC1	768.9	55.5	-1.9%
DC2	727.0	45.7	3.7%
DC3	702.6	33.4	6.9%
Impulse1	625.8	19.9	17.1%
Impulse2	679.0	67.3	10.0%
Impulse3	613.4	27.4	18.7%
Impulse+DC	215.6	41.5	71.4%

T.M. Harrell, O.T. Thomsen, J.M. Dulieu-Barton, and S.F. Madsen, “Damage in CFRP Composites Subjected to Simulated Lighting Strikes - Assessment of Thermal and Mechanical Responses,” Composites Part B: Engineering, 2019.
https://doi.org/10.1016/j.compositesb.2019.107298

Table 4. V-notch shear test results of control specimen and damaged specimens

Specimen	Mean Shear Strength [MPa]	Standard Deviation [MPa]	% Reduction
Control	87.6	0.70	-
DC1	83.6	1.02	4.5%
DC2	79.0	0.67	9.8%
DC3	81.1	3.13	7.4%
Impulse1	85.5	2.61	2.4%
Impulse2	80.5	4.18	8.1%
Impulse3	81.0	0.19	7.5%
Impulse+DC	49.9	0.67	43.0%

T.M. Harrell, O.T. Thomsen, J.M. Dulieu-Barton, and S.F. Madsen, “Damage in CFRP Composites Subjected to Simulated Lighting Strikes - Assessment of Thermal and Mechanical Responses,” Composites Part B: Engineering, 2019. https://doi.org/10.1016/j.compositesb.2019.107298

Table 5. Failure initiation stress for damaged shear samples

Specimen	Failure Initiation Stress [MPa] (mean)	Standard Deviation [MPa]	% Reduction
Control	16.2	0.82	-
DC1	12.3	0.20	24.2%
DC2	13.8	1.03	14.6%
DC3	12.7	1.13	21.5%
Impulse1	13.7	0.40	15.4%
Impulse2	13.0	0.27	19.7%
Impulse3	10.3	0.59	36.3%
Impulse+DC	6.4	1.77	60.8%